The Journal of Nutrition
Nutrition and Disease

Gestational Iron Deficiency Differentially Alters the Structure and Function of White and Gray Matter Brain Regions of Developing Rats[1–3]

Allison R. Greminger,[4–6] Dawn L. Lee,[4,6,7] Peter Shrager,[8] and Margot Mayer-Pröschel[6]*

Departments of [5]Environmental Medicine, [6]Biomedical Genetics, [7]Pathology and Laboratory Medicine, and [8]Neurobiology and Anatomy, University of Rochester, Rochester, NY

Abstract

Gestational iron deficiency (ID) has been associated with a wide variety of central nervous system (CNS) impairments in developing offspring. However, a focus on singular regions has impeded an understanding of the CNS-wide effects of this micronutrient deficiency. Because the developing brain requires iron during specific phases of growth in a region-specific manner, we hypothesized that maternal iron deprivation would lead to region-specific impairments in the CNS of offspring. Female rats were fed an iron control (Fe+) or iron-deficient (Fe−) diet containing 240 or 6 μg/g iron during gestation and lactation. The corpus callosum (CC), hippocampus, and cortex of the offspring were analyzed at postnatal day 21 (P21) and/or P40 using structural and functional measures. In the CC at P40, ID was associated with reduced peak amplitudes of compound action potentials specific to myelinated axons, in which diameters were reduced by ~20% compared with Fe+ controls. In the hippocampus, ID was associated with a 25% reduction in basal dendritic length of pyramidal neurons at P21, whereas branching complexity was unaffected. We also identified a shift toward increased proximal branching of apical dendrites in ID without an effect on overall length compared with Fe+ controls. ID also affected cortical neurons, but unlike the hippocampus, both apical and basal dendrites displayed a uniform decrease in branching complexity, with no significant effect on overall length. These deficits culminated in significantly poorer performance of P40 Fe− offspring in the novel object recognition task. Collectively, these results demonstrate that non-anemic gestational ID has a significant and region-specific impact on neuronal development and may provide a framework for understanding and recognizing the presentation of clinical symptoms of ID. J. Nutr. 144: 1058–1066, 2014.

Introduction

Iron is one of the most abundant metals on earth, yet deficiency in this essential metal continues to affect the health of pregnant women and children in virtually all nations and is associated with a vast number of behavioral, biochemical, and cellular defects in the developing central nervous system (CNS)[9] (1–9). The severity of impact that iron deficiency (ID) has on CNS development appears to correlate with the timing of onset, and studies in animal models and humans suggest that ID during the early stages of pregnancy is associated with impaired neuronal maturation and function (10–12). The cognitive impairments associated with these neuronal dysfunctions persist into adulthood despite iron supplementation, suggesting that ID causes permanent alterations of cellular structures and/or functions (13,14).

Although our understanding of the impact that ID has on brain function has grown considerably over the past decade, the use of various animal models and dietary protocols makes it challenging to compare data and gain a comprehensive picture of the full spectrum of impairments caused by gestational ID. The synonymous use of the terms ID and ID anemia (IDA) has hindered the study of 2 distinctly different pathologic states. IDA, the late-stage manifestation of chronic ID, is a common model used to study the developmental deficits caused by this micronutrient deficiency (15,16). However, IDA affects multiple organ systems and produces various secondary effects, complicating the assessment of how much of any observed neurologic defect is due to impaired hematopoiesis and subsequent hypoxia as opposed to the depletion of CNS iron stores. Although IDA has clear detrimental impacts on fetal development, the prevalence of ID without anemia is estimated to be 2.5 times greater and often remains undiagnosed because of the more subtle nature of its clinical symptoms and potential overlap with normal clinical

[1] Supported by NIH grants RO1 HD059739 and RO1 NS039511 and the University of Rochester through grants from the Clinical and Translational Science Institute and the Environmental Health Sciences Center.
[2] Author disclosures: A. R. Greminger, D. L. Lee, P. Shrager, and M. Mayer-Pröschel, no conflicts of interest.
[3] Supplemental Tables 1 and 2 are available from the "Online Supporting Material" link in the online posting of the article and from the same link in the online table of contents at http://jn.nutrition.org.
[4] A.R.G. and D.L.L. contributed equally to this work.
[9] Abbreviations used: AD, apical dendrite; AN, auditory nerve; BD, basal dendrite; CA1, cornu ammonis; CC, corpus callosum; CNS, central nervous system; Fe+, iron control; Fe−, iron-deficient; ID, iron deficiency; IDA, iron deficiency anemia; NOR, novel object recognition; P, postnatal day.
* To whom correspondence should be addressed. E-mail: Margot_Mayer-Proschel@urmc.rochester.edu.

Manuscript received November 1, 2013. Initial review completed December 12, 2013. Revision accepted March 21, 2014.
First published online April 17, 2014; doi:10.3945/jn.113.187732.

TABLE 1 Hematologic variables, brain iron concentration, and growth of iron-deficient and control rats during postnatal development[1]

	Fe+		Fe−		*P*		
	n	Value	*n*	Value	Age	Diet	Age × diet
Hematocrit, %					<0.001	<0.001	<0.001
P7	17	31.5 ± 1.19	14	29.2 ± 1.68			
P14	14	31.3 ± 1.19	10	30.1 ± 1.21			
P21	12	37.9 ± 1.17	15	23.2 ± 1.27*			
P40	23	44.4 ± 1.27	15	40.2 ± 1.57			
Hemoglobin, *g/dL*					0.001	0.03	0.82
P7	17	9.48 ± 0.56	14	8.47 ± 0.62			
P14	14	9.85 ± 1.24	10	8.23 ± 0.64			
P21	12	10.7 ± 0.72	15	9.75 ± 0.98			
P40	23	11.9 ± 1.02	15	11.2 ± 0.64			
MCH, *pg*					<0.001	0.69	0.30
P7	17	36.6 ± 1.02	14	35.3 ± 1.00			
P14	14	20.3 ± 0.85	10	23.4 ± 2.19			
P21	12	21.4 ± 0.73	15	22.4 ± 0.81			
P40	23	17.4 ± 0.98	15	16.2 ± 0.74			
MCV, *fL*					<0.001	0.07	0.62
P7	17	97.8 ± 1.72	14	94.3 ± 2.70			
P14	14	54.5 ± 3.03	10	55.4 ± 3.28			
P21	12	56.5 ± 3.35	15	46.2 ± 4.84			
P40	23	48.9 ± 2.62	15	43.6 ± 2.47			
Weight, *g*					<0.001	0.03	0.14
P7	25	9.73 ± 1.85	9	9.69 ± 1.1			
P14	16	19.2 ± 0.74	11	17.8 ± 0.43			
P21	11	27.6 ± 1.11	8	24.8 ± 0.86			
P40	16	91.6 ± 2.80	11	89.4 ± 2.29			
Brain iron, *μg/g*					0.03	<0.001	0.004
P7	4	14.8 ± 2.53	4	4.06 ± 2.2*			
P14	4	8.00 ± 1.00	4	6.91 ± 1.16			
P21	4	16.0 ± 1.16	4	7.29 ± 1.16*			
P40	4	14.4 ± 1.00	4	6.91 ± 1.00*			

[1] Results given as means ± SEMs; data represent 11–15 litters per diet group for weight and hematologic measurements and 4 litters per diet group for brain iron measurements, with *n* representing number of offspring used per diet group at each age. *$P < 0.05$, significantly different from age-matched control (Fe+). Fe+, iron control; Fe−, iron-deficient; MCH, mean corpuscular hemoglobin; MCV, mean corpuscular volume; P, postnatal day.

thresholds (17). Even if clearly defined models of ID, as opposed to IDA, are used to describe the impact on neuronal development, a focus on singular CNS regions makes it difficult to compare studies across the field and to understand its global impact on CNS development (11,18–26).

To generate a more comprehensive understanding of a possible CNS-wide phenotype in 1 defined system, we extended our previous studies on the auditory nerve (AN) (27) and examined another white matter tract, the corpus callosum (CC), as well as the hippocampus and cortex as functional gray matter regions. The inclusion of these gray matter regions allows for a direct comparison with the white matter impacts in the same animal model and a comparison with the data generated by others. Pathways from these regions are involved in various neurobehavioral circuits, and deficits in them may contribute to the behavioral deficits reported in iron-deficient children, reinforcing the need to study these regions in an integrated manner rather than singularly (28,29).

Given the highly variable demand and concentration of iron in specific regions of the brain and the resulting responses of various iron homeostasis proteins, it is likely that specific regions experience and exhibit diversity in their response to ID (30–32). The goal of this study was to establish whether multiple CNS regions show equal sensitivity to non-anemic gestational ID and to determine any temporal or regional specificity in sequalae.

Materials and Methods

Experimental design and diet administration. All protocols were approved by the University Committee on Animal Resources at the University of Rochester. Rats are from the same cohort as our previous publication, and handling and feeding paradigms are detailed there (27). Females were randomly assigned to diet group and fed an iron control (Fe+) or iron-deficient (Fe−) diet containing 240 μg/g (Harlan TD 05656) or 6 μg/g (Harlan TD80396) iron, respectively, for 2 wk before mating and throughout gestation/lactation. All diets were purchased from Teklad Lab Animal Diets, Harlan Laboratories (for diet formulation and nutritional components, see **Supplemental Table 1**). Offspring were weaned onto the same diet as their respective dams and were designated as the Fe+ group (total of 15 litters) and Fe− group (total of 13 litters), respectively. Only 1 male and 1 female from a single litter were included in any 1 age group per endpoint to control for litter-specific effects, except for measurements of postnatal weight and hematologic indices of **Table 1**, in which some litters were sampled more than once. The number of offspring per group or per age is represented by *n* (for numbers of litters used per endpoint, see table and figure legends). Analyses were performed on offspring of mixed sex, with equal numbers of each sex used per endpoint, when

possible. Postnatal growth of this cohort, hematologic measures, and whole-brain iron measurements were performed as described previously (27) and were compared using the definitions of anemia set forward by the WHO (33,34).

Tissue harvest and Western blotting. Rats were asphyxiated with carbon dioxide at postnatal day 7 (P7), P14, P21, and P40, and brain tissue was processed as described previously (27). Briefly, 40 μg of protein was resolved by SDS-PAGE, and membranes were probed for anti-ferritin heavy chain (Cell Signaling Technology), using β-actin as a loading control. Immunoreactive proteins were detected and quantified by densitometry as described previously (27).

Electron microscopy. Electron microscopy analysis was conducted on P40 offspring. Rats were deeply anesthetized and perfused with fixative as described previously (27,35). Slices, 1 mm thick, were made of the postfixed brains to expose the CC and were submitted for ultrathin sectioning. All samples were osmicated, stained, dehydrated, and embedded in resin as described previously (27,35). A minimum of 5 images were captured for each tissue sample at 5000× magnification and used for axon diameter and myelin thickness measurements and at 70,000× magnification for counts of lamellae.

EM quantitative analysis. Axon density was determined by counting the number of axons in 9 different 25-μm^2 areas in each of the 5 photomicrographs using the cell counter function in NIH ImageJ. Axon diameter (the inner diameter of the myelin sheath), myelin thickness (defined as myelinated fiber diameter minus axon diameter), and percentage of myelination were determined by measuring all axons contained in the same 9 25-μm^2 areas of interest used in the density measurement. Approximately 1000 axons were measured per rat, and only fibers cut transversely were measured. The same systematic sampling was used for all samples, and photomicrographs were coded and analyzed blindly to avoid bias.

Electrophysiologic recording procedures. Electrophysiology was conducted on P40 offspring to correlate to previous electrophysiology measures conducted at P40 in the AN (27). The CC was prepared as described previously, and electrophysiologic recording procedures were adapted from Reeves et al. (35). In our experiments, the recording electrode was later repositioned from the initial distance of 1.6 mm to distances of 1.2, 1.0, and 0.6 mm. More than 90% of the stimulus artifact was subtracted by placing a second recording pipette electrode in the bath and feeding both signals into a differential amplifier of our own design. Evoked action potentials were amplified (bandpass: direct current to 10 kHz) and digitized at 25–100 kHz. Quantification of mean latency in milliseconds and absolute amplitude in millivolts was calculated based on time to each peak and height of each peak, respectively.

Golgi-Cox staining. Brains of P21 offspring were placed directly into Golgi solution, stored, and prepared for sectioning as described previously (11). This age was chosen for Golgi analysis, because this is the time point at which pyramidal neurons first stabilize after a period of rapid changes during development (36). Approximately 24 midsagittal plane sections of 150 μm thickness per brain were collected from a Leica vibratome (VT1000S; Leica Biosystems). Sections were reacted in ammonium hydroxide and sodium thiosulfate solution as described previously (11). Neuron tracings were done on an Olympus DSU BX51WI microscope (Olympus America) and captured using an MBF CX9000 digital camera with Neurolucida software (MBF Biosciences). Randomly selected pyramidal neurons were traced at 40× or 100× from the cornu ammonis (CA1) hippocampus region and layers 3–4 (~400 μm from the dorsal surface) of the frontal cortex on each slide. Dendritic tracing was performed as described previously (11).

Morphometric analysis. Sholl analysis was conducted and analyzed as described previously (11,37). The Neurolucida software provided overall neuron summary information, including mean dendritic length, branch order, and ring crossings calibrated to distance from soma. Extent of branching was assessed by counting the number of intersections at each of the Sholl rings. Total crossings at each ring within apical and basal dendrite (BD) subdivisions for each neuron were recorded. Peak branching distance was defined as described previously (11). For all analysis, individual neurons were averaged per rat and then per group.

Novel object recognition task. The behavioral novel object recognition (NOR) test is used to assess recognition memory in rodent models and was performed as described previously (38–40). Offspring were allowed to freely explore the empty arena (70 × 70 × 9 cm) for 10 min on day 1. The next day, the rats were placed in the arena with 2 identical objects for 10 min to facilitate familiarization. On the last day, the rats were placed in the arena with 1 familiar object and 1 novel sample object. Objects selected for NOR testing were cleaned with 70% ethanol to eliminate residual scent between rats. The CleverSys tracking system (CleverSys) measured the time spent interacting with the objects. Object interaction was defined as entrance in the object-containing zone (5 cm radius) resulting in direct or nearly direct object contact with the nose or whiskers. All rats were returned to their home cages between test trial phases. The time spent exploring each object and the discrimination index percentage were quantified from digital recordings.

Statistical analysis. Statistical comparisons of densitometry were performed by ANOVA (diet × age). Electrophysiology results in the CC were analyzed by ANOVA (diet × electrode distance). Axon diameter distribution in the CC was analyzed by ANOVA (diet × diameter). The number of intersections measured in the Sholl analysis was analyzed by ANOVA (diet × distance from soma). For statistically significant main effects or interactions, post hoc Holm-Sidak tests were used to compare Fe− to Fe+ offspring at each time point or secondary factor (e.g., diameter, distance), using SigmaPlot 11 (Systat Software). Student's *t* test was used for comparisons of overall dendritic length (data not shown), axon diameter, and CC axonal characteristics (**Supplemental Table 2**) for the Fe+ and Fe− groups. A P value <0.05 was considered statistically significant.

Results

Postnatal growth and hematologic measures. In general, Fe− rats had similar growth patterns during postnatal development compared with the Fe+ group, excluding overt malnutrition (Table 1). For postnatal weight, there was an effect of age ($P < 0.001$) and diet ($P < 0.04$) but no age × diet interaction ($P = 0.14$). Hematologic measures and whole-brain iron measurement were conducted as described previously (27) and showed a significant decrease in hematocrit at P21 in the ID cohort that was not associated with a change in hemoglobin concentrations or other hematologic variables. We did not see significant diet × age interactions in hematologic variables at any other ages (Table 1).

CC iron stores and axonal structure. Overall, there was a significant effect of diet ($P < 0.005$) on CC cellular iron stores measured by ferritin protein concentrations but no diet × age interactions. Ferritin expression was decreased by ~25% in the Fe− group compared with Fe+ controls across older ages (**Fig. 1***A*). At P40, myelinated axon diameter was significantly greater in the Fe+ group (0.60 ± 0.03 μm) compared with Fe− offspring (0.49 ± 0.02 μm) ($P = 0.03$), whereas the diameter of non-myelinated axons was unaffected ($P = 0.12$) (Fig. 1*C*). This age was chosen because the CC showed significant signs of tissue ID and allowed a correlation with the deficits observed previously at P40 in the AN (27). When displayed as a frequency across diameter, there was an effect of diameter ($P < 0.001$), representing the bell-shaped distribution (Fig. 1*D*). There was a significant diet × diameter interaction ($P < 0.001$), indicating that diet did not have a uniform effect across all sizes of diameter. Specifically, the frequency of small axons, 0.5μm in diameter, was significantly

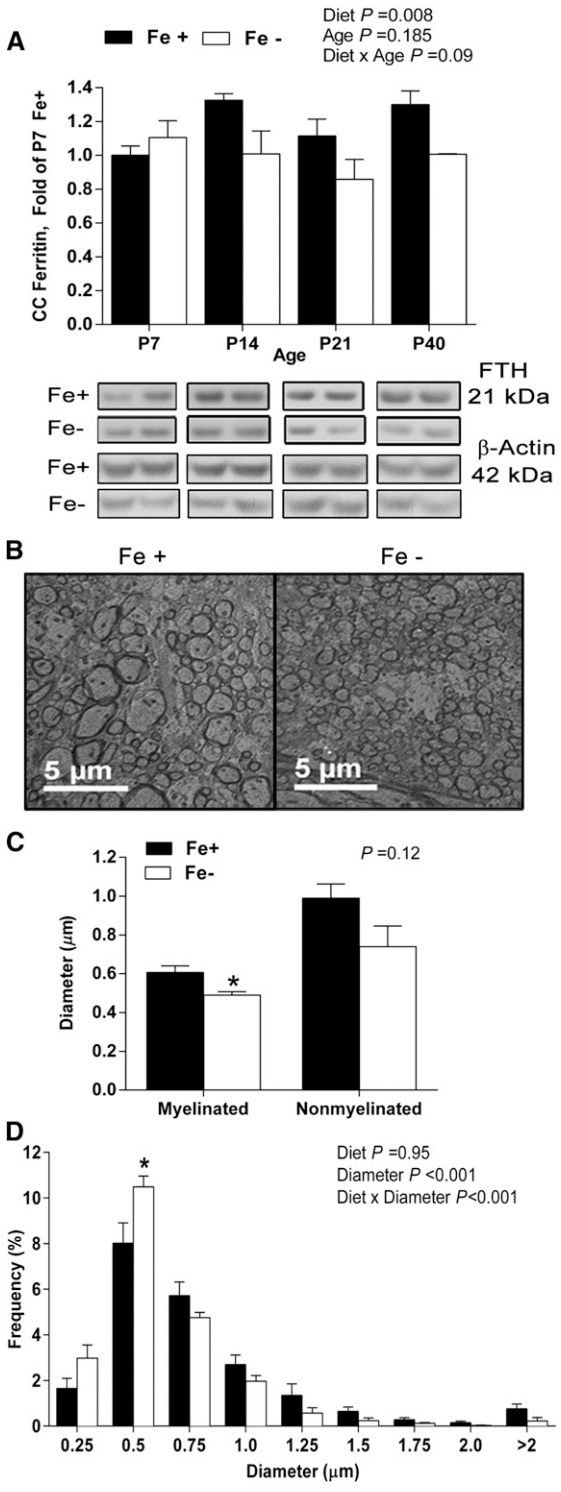

FIGURE 1 Tissue ferritin protein concentrations and axonal structural characteristics of CC from Fe+ and Fe− rats. Ferritin expression in CC lysates from Fe+ and Fe− rats normalized to the P7 Fe+ amount; representative Western bands are shown below each age for each diet group (*A*). Data represent 9–10 total litters per diet group, with $n = 6$ rats per age per diet group. Representative electron micrographs from P40 Fe+ and Fe− CC at 2500× (*B*). Mean axon diameter of myelinated and nonmyelinated fibers; $*P < 0.05$, Fe+ vs. Fe− by Student's *t* test (*C*). Axon diameter distribution of axons in P40 Fe+ or Fe− CC; $*P < 0.05$, Fe+ vs. Fe− within axon diameter (*D*). Data represent 3 total litters per diet group, with $n = 3$ rats per diet group. Values are means ± SEMs. CC, corpus callosum; Fe+, iron control; Fe−, iron-deficient; FTH, ferritin heavy chain; P, postnatal day.

higher for the Fe− group (10.9 ± 0.40%) than the Fe+ group (8.39 ± 0.87%) ($P < 0.05$). There were no significant diet group differences in CC axonal density, ruling out simple changes in the total number of axons (Supplemental Table 2). Additionally, there were no significant diet group differences in myelin thickness, calculated *g* ratio (Supplemental Table 2), or protein concentrations of myelin constituents, including myelin basic protein, or myelin associated glycoprotein (data not shown).

CC compound action potential electrophysiology. Brain slice compound action potential electrophysiologic recordings are characterized by 2 waveform components generated by myelinated axons (N1 wave) and nonmyelinated axons (N2 wave) (**Fig. 2***A*) (35,41,42). Overall, there was a significant effect of stimulus distance ($P < 0.001$), and waveform amplitudes decreased as stimulus distance increased. For N1 waveforms, there was a significant main effect of diet ($P < 0.001$), and N1 wave amplitudes were marginally smaller in the Fe− group across all stimulus distances compared with the Fe+ group (Fig. 2*B*). In contrast, there were no significant diet group differences in callosal N2 waveforms ($P = 0.75$) (Fig. 2*C*). When amplitude was expressed as a ratio of N1-to-N2 waveforms, there was a significant effect of diet ($P < 0.001$), and amplitudes were decreased by 25–50% in the Fe− diet group compared with the Fe+ diet group across stimulus distance. For the ratio, there was also an effect of stimulus distance ($P < 0.001$) (Fig. 2*D*). There were no significant diet group differences in conduction velocity for either the N1 or N2 waveforms (data not shown).

Iron store mobilization in gray matter regions. For the hippocampus, there was an effect of diet ($P < 0.001$), age ($P = 0.04$), and diet × age interaction ($P < 0.001$). Ferritin protein expression in the hippocampus of the Fe− diet group was significantly less than that of the Fe+ diet group at P14 (~60% less), P21 (~35%), and P40 (~25%) ($P < 0.05$) (**Fig. 3***A*). Within the Fe+ diet group, ferritin expression was significantly increased at P14 (~70%) and decreased at P21 (~30%) and P40 (~20%) compared with P7 ($P < 0.05$). Within the Fe− diet group, ferritin expression was significantly decreased at P14 (~30%), P21 (~50%), and P40 (~40%) compared with P7 ($P < 0.05$). In the cortex, there was a significant effect of diet ($P < 0.001$), age ($P < 0.001$), and diet × age interaction ($P = 0.04$). Ferritin protein expression in the cortex of the Fe− diet group was significantly less than that of the Fe+ diet group at P14 (~50%) and P40 (~40%) ($P < 0.05$) (Fig. 3*B*). Within the Fe+ diet group, ferritin expression was significantly increased at P14 (~100%) ($P < 0.05$), whereas expression was similar at all ages within the Fe− group.

Dendritic complexity of hippocampal pyramidal neurons. Multiple discrepancies in hippocampal dendritic arborization were observed between both diet groups at P21, and representative images from the CA1 region are shown in **Figure 4***A*.

BD length was significantly shorter ($P = 0.01$) in Fe− CA1 pyramidal neurons compared with those of the Fe+ diet group (data not shown). In contrast, apical dendrite (AD) length was not significantly affected by diet group ($P = 0.05$) (data not shown). For BD complexity, by analysis of Sholl ring intersections, there was a significant effect of distance from the soma ($P < 0.001$), indicating a decrease in complexity with increasing distance from the soma, a profile reported previously (11,43). Slight decreases in the number of BD Sholl ring intersections were observed in the Fe− group around 150 µm from the soma, although there were no significant effects of diet ($P = 0.10$) or diet × age interactions ($P = 0.93$) (Fig. 4*B*). Sholl analysis of AD

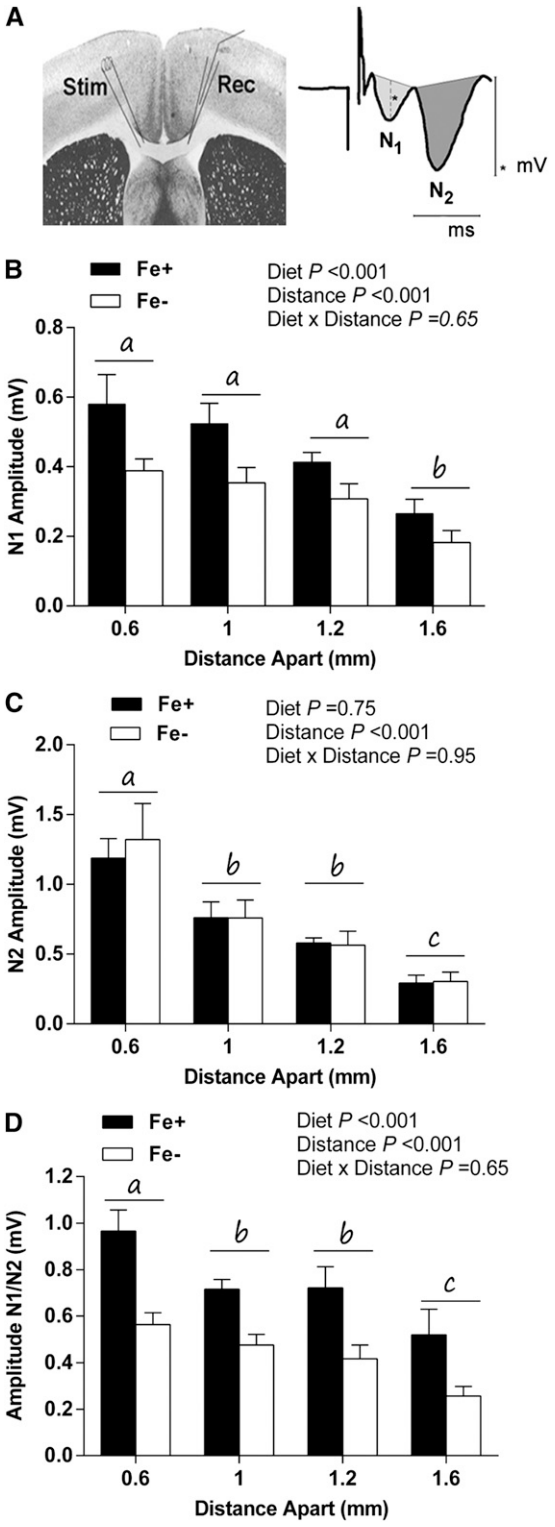

FIGURE 2 Electrophysiology of postnatal day 40 CC in Fe+ and Fe− rats. Schematic of stimulating and recording electrode placements (left), representative compound action potential waveform (right), and illustrative quantification of N1 and N2 waveforms (*A*). *indicates measure of amplitude. Mean N1 wave amplitude across stimulus distance (*B*). Mean N2 amplitude across stimulus distance (*C*). Ratio of N1-to-N2 waveform amplitude across stimulus distance (*D*). Distances without a common letter differ significantly ($P < 0.05$). Values are means ± SEMs. Data represent 4–5 litters per group, with $n = 5$ for the Fe+ group and 4 for the Fe− group. CC, corpus callosum; Fe+, iron control; Fe−, iron-deficient; Rec, recording electrode; N1, myelinated axons; N2, nonmyelinated axons; Stim, stimulating electrode.

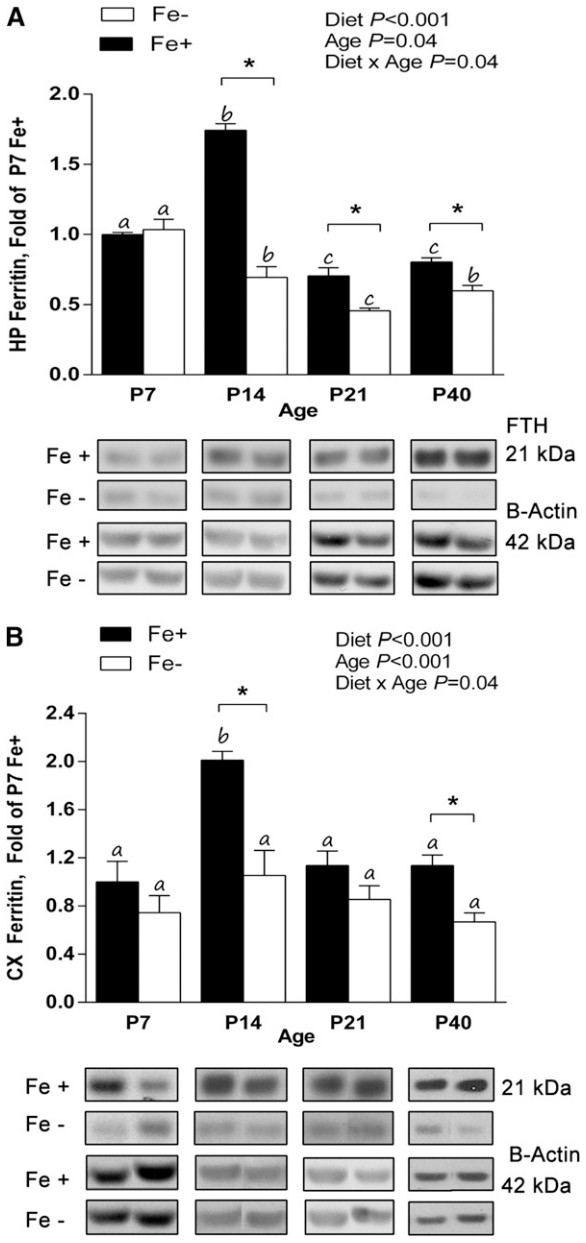

FIGURE 3 Ferritin protein concentrations in the HP and CX of Fe+ and Fe− offspring during development. Ferritin expression in P7, P14, P21, and P40 HP (*A*) and P40 CX lysates from Fe+ and Fe− rats normalized to P7 Fe+ (*B*). Within each diet group, ages without a common letter differ significantly ($P < 0.05$). *$P < 0.05$, significantly different from age-matched Fe+ group. Values are means ± SEMs. For HP, data represent 9–10 total litters per diet group, with $n = 6$ rats per age per diet. For CX, data represent 14–15 total litters per diet group, with $n = 6$ rats per age per diet. CX, cortex; Fe+, iron control; Fe−, iron-deficient; FTH, ferritin heavy chain; HP, hippocampus; P, postnatal day.

complexity revealed a significant effect of diet ($P = 0.02$), distance ($P < 0.001$), and a diet × distance interaction ($P < 0.001$). The AD of the Fe− diet group displayed increased proximal and decreased distal branching compared with the Fe+ group. The number of intersections was significantly fewer (~50% fewer) in the Fe− group at distances of 200 and 210 μm compared with Fe+ AD ($P < 0.05$) (Fig. 4*C*). There were no significant diet effects on quantity of BD ($P = 0.79$), AD ($P = 0.59$), or soma surface area ($P = 0.46$), indicating primarily a geographical deviation in branching of dendrites in the Fe− diet group.

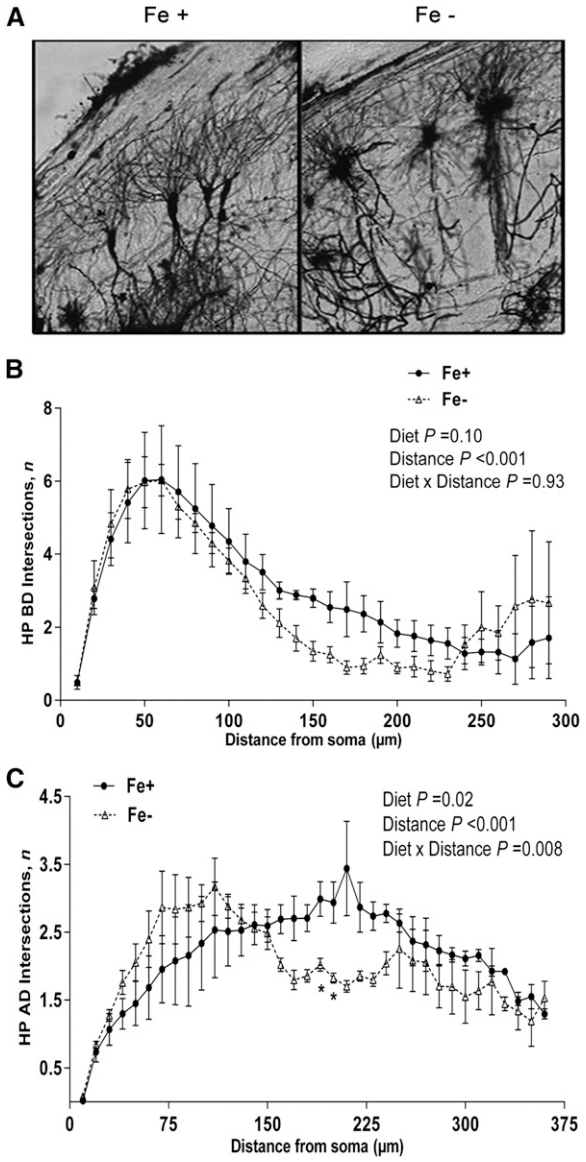

FIGURE 4 Golgi staining and Sholl analysis of branching complexity of HP dendritic populations from postnatal day 21 Fe+ and Fe− rats. Representative images (10×) of Golgi–Cox-stained pyramidal neurons from HP CA1 sections of Fe+ and Fe− rats (*A*). Number of Sholl ring intersections of BD (*B*) and AD (*C*) of HP neurons from Fe+ and Fe− rats. $*P < 0.05$, vs. Fe+ at specified distance from the soma. Values are means ± SEMs. Data represent 4 independent litters per diet group, with $n = 4$ rats per age per group. AD, apical dendrite; BD, basal dendrite; Fe+, iron control; Fe−, iron-deficient; HP, hippocampus.

Dendritic complexity of cortical neurons. There was no significant effect of diet on overall length of ADs ($P = 0.10$) or BDs ($P = 0.05$) (data not shown). Whereas alterations in the hippocampus were distinct between dendritic subpopulations, the overall distribution pattern of branching in the cortex was similar between both dendritic subpopulations. For BD, there was a significant effect of diet ($P < 0.001$) such that the Fe− group displayed fewer branches at proximal distances (**Fig. 5***B*). There was also an effect of distance from the soma ($P < 0.001$) but no diet × distance interaction ($P = 0.37$). For AD, there was a significant effect of diet ($P < 0.001$), and the Fe− group displayed decreased proximal branching that was most evident at distances <100 μm from the soma (Fig. 5*C*). An effect of distance ($P < 0.001$) was also observed in this dendritic population, but there was no diet × distance interaction ($P = 0.79$).

NOR task. Exploration time was marginally longer for the novel object in offspring of the Fe+ group ($P = 0.09$), whereas Fe− rats spent equal amounts of time exploring both old and novel objects ($P = 0.99$) (**Fig. 6***A*). The discrimination index (ratio of time spent exploring novel-to-old objects) was also significantly higher ($P = 0.02$) in the Fe+ group and exceeded that of the Fe− group by ~20% (Fig. 6*B*).

Discussion

This study provides evidence that gestational non-anemic ID is associated with impairments in cellular processes of white and gray matter regions in the developing CNS. Specifically, we show the following. *1*) ID does not have to reach the level of anemia to

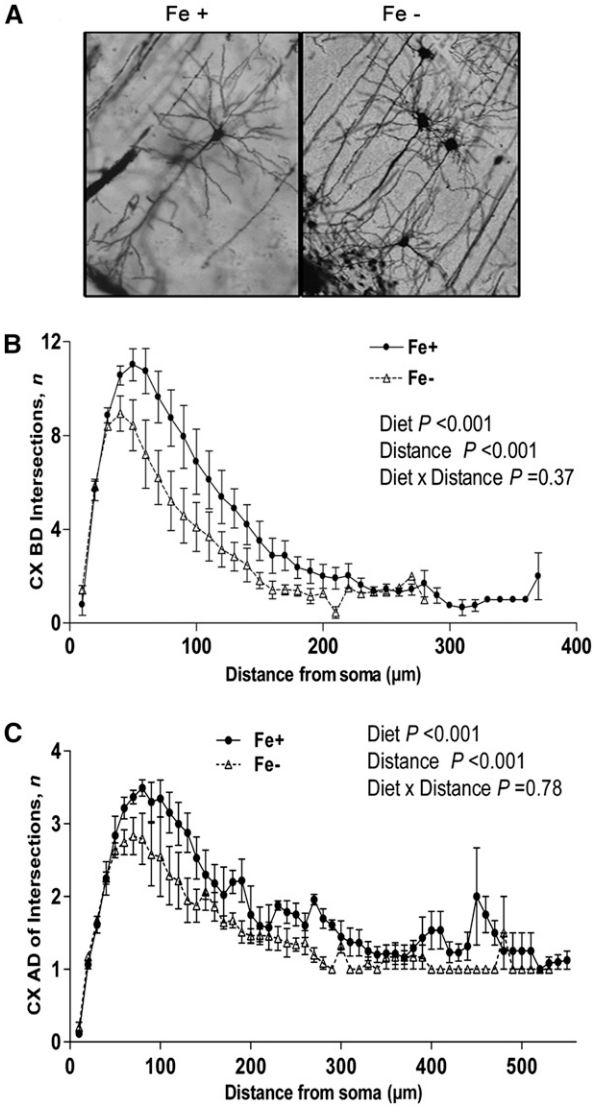

FIGURE 5 Golgi staining and Sholl analysis of branching complexity of CX dendritic populations from postnatal day 21 Fe+ and Fe− rats. Representative images (20×) of Golgi–Cox-stained CX neurons from Fe+ and Fe− rats (*A*). Number of Sholl ring intersections of BD (*B*) and AD (*C*) from Fe+ and Fe− CX neurons. Values are as means ± SEMs. Data represent 4 independent litters per diet group, with $n = 4$ rats per age per group. AD, apical dendrite; BD, basal dendrite; CX, cortex; Fe+, iron control; Fe−, iron-deficient.

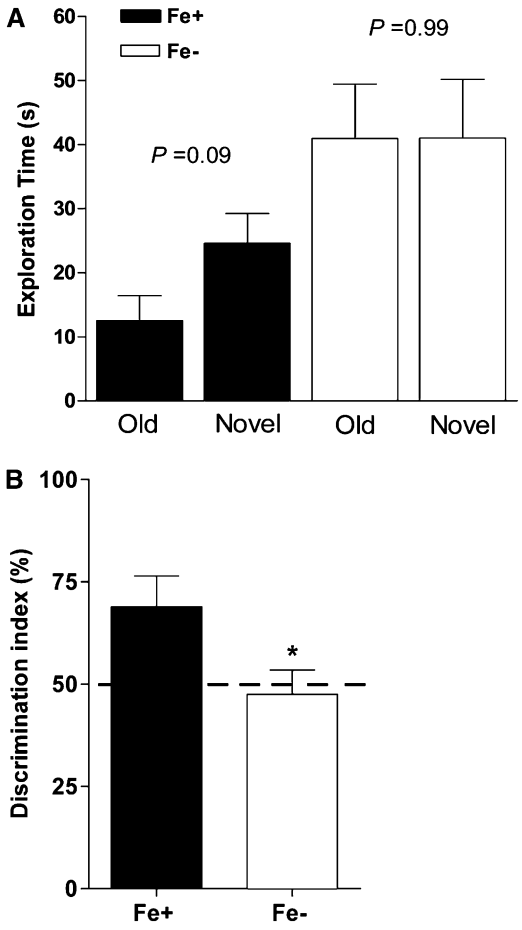

FIGURE 6 NOR task performance of postnatal day 40 Fe+ and Fe− rats. Exploration time spent on old vs. novel objects in the NOR arena by Fe+ and Fe− rats (*A*). Percentage of total exploration time spent with novel object (discrimination index) during session of Fe+ and Fe− rats (*B*). $*P < 0.05$ vs. Fe+. Dashed line indicates the threshold for preference between test objects. Values are means ± SEMs. Data represent 6 total litters per diet group, with $n = 6$ rats per group. Fe+, iron control; Fe−, iron-deficient; NOR, novel object recognition.

have a profound impact on both white and gray matter regions. *2*) The depletion of tissue iron, measured by ferritin concentrations, is not uniform across the CNS and occurs earlier in gray matter than in white matter regions. *3*) The impact of ID without anemia on axonal architecture and maturation is more profound than the impact on myelination, and *4*) functional impairments are characterized by alterations in neuronal structure. Together, these data suggest that ID-induced alterations are not benign, and the impact of ID on CNS function is best studied in a manner that takes into account these regional differences.

An important aspect of our study is the focus on ID that is initiated before gestation and is sustained throughout the life of the offspring at an amount that does not cause anemia but is significant enough to initiate changes in tissue iron homeostasis. This mimics a situation that is likely to be prevalent in humans, in which tissue ID occurs early in development but does not cause clinical signs of anemia and would hence not prompt immediate iron supplementation. Our data show that even non-anemic ID has a significant impact on multiple CNS regions leading to functional impairment. The effectiveness of iron supplementation on reversing these deficits is an intriguing question in light of studies that show that correction of the hematologic variables of ID does not benefit the CNS (2,8,13,26,44,45). Work from our own laboratory confirmed the presence of a gestational window of vulnerability (33).

Our analysis of the CC, the largest white matter tract in the brain, highlights the regional specificity of ID (46). This myelinated tract is responsible for interhemispheric connectivity, and deficits in its function could contribute to poorer cognitive performance or behavioral abnormalities that were reported with IDA. We observed a significant decrease in axonal diameter of myelinated axons in Fe− offspring. This was not a result of hypermyelination of small-diameter axons at the cost of larger-diameter axons, because the *g* ratio (Supplemental Table 2) was preserved in the Fe− group, indicating normal myelination of all axons. The differential vulnerability of myelinated axons in this white matter tract could be consistent with disruptions in myelination or axon–glial interactions during development. However, the myelin protein profile of the CC was not altered by diet, and ultrastructural analysis revealed no gross myelin abnormalities. These data would suggest then that there is no intrinsic myelin deficit but that axons may not be responding properly to glial-generated cues in regulation of diameter size. This possible miscommunication in the iron-deficient CC may be sufficient to prevent the recruitment of these fibers into the compound action potential field.

Interestingly, the decreases in myelinated axon diameter were not accompanied by significant decreases in signal conduction velocity but were instead associated with a significant decrease in signal strength (indicated by decreased amplitude). When we compared the results from the CC with those in the AN (27), it appears that different mechanisms contribute to the functional deficits produced by decreased axonal diameter. Although decreases in axonal diameter were sufficient to impede the speed of action potential propagation in the AN, the same structural changes only affected action potential signal strength, not speed in the CC. This indicates that the regional hierarchy of susceptibility to ID extends to the underlying mechanisms, the specifics of which are as yet unknown.

The specific impairments we identified were mainly associated with neuronal maturation rather than any glial dysfunctions. This is consistent with our previous study of mild ID on the AN, in which we did not see a myelination defect (27). However, this is in contrast to studies using models of IDA, in which profound myelination defects are seen (45,47,48). This suggests that the prevalent defects in myelination are most likely due to the secondary effects of anemia, including ischemia, hypoxia, or concurrent hypothyroidism rather than deficiencies in iron alone (8,49,50). Although it is true that oligodendrocytes require iron as a cofactor in enzymes that produce myelin, studies that reported hypomyelination used a more severe ID or anemia (with decreases in hematocrit averaging 50% less than age-matched controls) compared with our feeding paradigm (47,48,51,52).

Our study of hippocampal and cortical tissues extends and supports reports from others showing that the gray matter is affected by even mild ID (11,25–27,32). A detailed structural characterization including Sholl analyses revealed significant impairments in dendritic arborization and organization at P21. This time point occurs shortly after the first signs of tissue ID in the hippocampus (Fig. 3) and thus allowed us to look at the acute structural effects of developmental ID. The decrease in hippocampal ferritin expression is maintained through P40 despite an increase in hematocrit concentrations during this time, which would suggest that the effects of ID at P21 might actually underestimate any effects that would be present at P40. Georgieff and colleagues (10,11,25,53) extensively described ID-induced alterations in hippocampal neuronal architecture and associated

impairments in neuronal function. From these studies, it has become clear that sufficient iron stores are critical for accurate dendritic arborization in the hippocampus. In agreement with these data, we discovered proximal shifts in AD branching and identified decreases in BD length and branching, a defect not described previously. The hippocampus is a critical component of recognition memory, and knockouts of proteins involved in proper synaptic signaling, injury/lesion models, and pharmacologic drugs that inhibit hippocampal function resulted in reproducible deficits in rodent performance of the NOR task (35–37). This connection seems likely given the structural changes in the hippocampus and decreased novel object exploration in Fe− offspring. Although untested here, it is probable that the defects uncovered on the morphologic level would also result in reduced long-term potentiation and elevated paired-pulse facilitation as shown previously and impaired prepulse inhibition as described recently by Pisansky and colleagues (19,54).

Our investigation of the morphological alterations in the cortex emphasizes the region-specific impact of ID on neuronal structure. The shift in peak branching distance observed in the hippocampus did not predict the morphological alterations we revealed in the cortex, in which the abnormalities in dendritic branching were similar in both the apical and basal subdivisions. These findings in the cortex are novel and suggest that ID could interfere with the connectivity between the hippocampus and cortex, impeding circuits designed to encode spatial and other episodic memories (55,56). This is supported by studies showing that lesions of the enterorhinal cortex disrupted object recognition memory in monkeys, implicating a critical function of both the cortex itself and its connectivity with the hippocampus in the NOR task (57). These alterations in the pattern of dendritic complexity and possible impact on signaling may precipitate the poorer performance of Fe− rats in the NOR task and mimic results reported in other animal models of ID, as well as in iron-deficient children (2,10).

Our analysis of multiple brain regions in a cohort of rats that were fed identical diets (except for iron content) has allowed additional new insights and confirms the variability of the impact of ID on neurodevelopment. We found that the degree of impairment between different regions in the same rat was more variable than the degree of impairment across different rats, suggesting a uniform hierarchy of regional susceptibility. We confirmed that iron depletion occurs in a region-specific manner and that individual CNS regions display differential vulnerability to molecular and functional deficits, which coincides with published literature that reported regional differences in iron homeostasis proteins and deficits in isolated regions. However, our study reinforces the fact that it is the integration of all these regions that is critical for proper CNS development and that this phenomenon remains understudied in nutritional deficiencies.

Acknowledgments

The authors thank Ollivier Hyrien for assistance in the statistical evaluation of our data and Gayle Schneider and Kathryn Hutton for excellent technical assistance. They also thank Karen Bentley for her assistance with the electron microscopy analysis. The authors thank Jacob Mitchell, Joshua Levy, and Christopher Hoeger, who were involved in the Golgi analysis, as well as Fred Strathman, Mark Noble, and Chris Pröschel for their support and insights. D.L.L., A.R.G., P.S., and M.M.-P. designed the research; D.L.L. and A.R.G. performed the research; D.L.L. and A.R.G. analyzed the data; and D.L.L., A.R.G., P.S., and M.M.-P. wrote the paper. All authors read and approved the final manuscript.

References

1. Lozoff B. Early iron deficiency has brain and behavior effects consistent with dopaminergic dysfunction. J Nutr. 2011;141:740S–6S.
2. Lukowski AF, Koss M, Burden MJ, Jonides J, Nelson CA, Kaciroti N, Jimenez E, Lozoff B. Iron deficiency in infancy and neurocognitive functioning at 19 years: evidence of long-term deficits in executive function and recognition memory. Nutr Neurosci. 2010;13:54–70.
3. Carter RC, Jacobson JL, Burden MJ, Armony-Sivan R, Dodge NC, Angelilli ML, Lozoff B, Jacobson SW. Iron deficiency anemia and cognitive function in infancy. Pediatrics. 2010;126:e427–34.
4. Shafir T, Angulo-Barroso R, Jing Y, Angelilli ML, Jacobson SW, Lozoff B. Iron deficiency and infant motor development. Early Hum Dev. 2008;84:479–85.
5. Lozoff B, Clark KM, Jing Y, Armony-Sivan R, Angelilli ML, Jacobson SW: Dose-response relationships between iron deficiency with or without anemia and infant social-emotional behavior. J Pediatr. 2008; 152:696–702, 702.31–3.
6. Walker SP, Wachs TD, Gardner JM, Lozoff B, Wasserman GA, Pollitt E, Carter JA. Child development: risk factors for adverse outcomes in developing countries. Lancet. 2007;369:145–57.
7. Lozoff B. Iron deficiency and child development. Food Nutr Bull. 2007; 28:S560–71.
8. Algarín C, Peirano P, Garrido M, Pizarro F, Lozoff B. Iron deficiency anemia in infancy: long-lasting effects on auditory and visual system functioning. Pediatr Res. 2003;53:217–23.
9. Roncagliolo M, Garrido M, Walter T, Peirano P, Lozoff B. Evidence of altered central nervous system development in infants with iron deficiency anemia at 6mo: delayed maturation of auditory brainstem responses. Am J Clin Nutr. 1998;68:683–90.
10. Georgieff MK. The role of iron in neurodevelopment: fetal iron deficiency and the developing hippocampus. Biochem Soc Trans. 2008;36:1267–71.
11. Brunette KE, Tran PV, Wobken JD, Carlson ES, Georgieff MK. Gestational and neonatal iron deficiency alters apical dendrite structure of CA1 pyramidal neurons in adult rat hippocampus. Dev Neurosci. 2010;32:238–48.
12. Dallman PR. Biochemical basis for the manifestations of iron deficiency. Annu Rev Nutr. 1986;6:13–40.
13. Lozoff B, Jimenez E, Hagen J, Mollen E, Wolf AW. Poorer behavioral and developmental outcome more than 10 years after treatment for iron deficiency in infancy. Pediatrics. 2000;105:E51.
14. Felt BT, Lozoff B. Brain iron and behavior of rats are not normalized by treatment of iron deficiency anemia during early development. J Nutr. 1996;126:693–701.
15. Scholl TO. Maternal iron status: relation to fetal growth, length of gestation, and iron endowment of the neonate. Nutr Rev. 2011;69:S23–9.
16. Scholl TO. Iron status during pregnancy: setting the stage for mother and infant. Am J Clin Nutr. 2005;81:1218S–22S.
17. World Health Organization. Iron deficiency anaemia: assessment, prevention and control: a guide for program managers. Vol. 2011. Geneva, Switzerland: WHO; 2001.
18. Rao R, Tkac I, Unger EL, Ennis K, Hurst A, Schallert T, Connor J, Felt B, Georgieff MK. Iron supplementation dose for perinatal iron deficiency differentially alters the neurochemistry of the frontal cortex and hippocampus in adult rats. Pediatr Res. 2013;73:31–7.
19. Pisansky MT, Wickham RJ, Su J, Fretham S, Yuan LL, Sun M, Gewirtz JC, Georgieff MK. Iron deficiency with or without anemia impairs prepulse inhibition of the startle reflex. Hippocampus. 2013; June 3 (Epub ahead of print; DOI:10.1002/hipo.22151).
20. Fretham SJ, Carlson ES, Georgieff MK. Neuronal-specific iron deficiency dysregulates mammalian target of rapamycin signaling during hippocampal development in nonanemic genetic mouse models. J Nutr. 2013;143:260–6.
21. Unger EL, Hurst AR, Georgieff MK, Schallert T, Rao R, Connor JR, Kaciroti N, Lozoff B, Felt B. Behavior and monoamine deficits in prenatal and perinatal iron deficiency are not corrected by early postnatal moderate-iron or high-iron diets in rats. J Nutr. 2012;142:2040–9.
22. Tran PV, Fretham SJB, Wobken J, Miller BS, Georgieff MK. Gestational-neonatal iron deficiency suppresses and iron treatment reactivates IGF signaling in developing rat hippocampus. Am J Physiol Endocrinol Metab. 2012;302:E316–24.
23. Fuglestad AJ, Georgieff MK, Iverson SL, Miller BS, Petryk A, Johnson DE, Kroupina MG. Iron deficiency after arrival is associated with general cognitive and behavioral impairment in post-institutionalized children adopted from Eastern Europe. Matern Child Health J. 2013;17:1080–7.

24. Bastian TW, Anderson JA, Fretham SJ, Prohaska JR, Georgieff MK, Anderson GW. Fetal and neonatal iron deficiency reduces thyroid hormone-responsive gene mRNA levels in the neonatal rat hippocampus and cerebral cortex. Endocrinology. 2012;153:5668–80.
25. Rao R, Tkac I, Schmidt AT, Georgieff MK. Fetal and neonatal iron deficiency causes volume loss and alters the neurochemical profile of the adult rat hippocampus. Nutr Neurosci. 2011;14:59–65.
26. Tran PV, Fretham SJ, Carlson ES, Georgieff MK. Long-term reduction of hippocampal brain-derived neurotrophic factor activity after fetal-neonatal iron deficiency in adult rats. Pediatr Res. 2009;65:493–8.
27. Lee DL, Strathmann FG, Gelein R, Walton J, Mayer-Proschel M. Iron deficiency disrupts axon maturation of the developing auditory nerve. J Neurosci. 2012;32:5010–5.
28. Siddappa AM, Georgieff MK, Wewerka S, Worwa C, Nelson CA, Deregnier RA. Iron deficiency alters auditory recognition memory in newborn infants of diabetic mothers. Pediatr Res. 2004;55:1034–41.
29. Youdim MB. Brain iron deficiency and excess; cognitive impairment and neurodegeneration with involvement of striatum and hippocampus. Neurotox Res. 2008;14:45–56.
30. Beard JL, Connor JR, Jones BC. Iron in the Brain. Nutr Rev. 1993;51: 157–70.
31. Focht SJ, Snyder BS, Beard JL, Van Gelder W, Williams LR, Connor JR. Regional distribution of iron, transferrin, ferritin, and oxidatively-modified proteins in young and aged Fischer 344 rat brains. Neuroscience. 1997;79:255–61.
32. Erikson KM, Pinero D, Connor J, Beard JL. Regional brain iron, ferritin and transferrin concentrations during iron deficiency and iron repletion in developing rats. J Nutr. 1997;127:2030–8.
33. Mihaila C, Schramm J, Strathmann FG, Lee DL, Gelein RM, Luebke AE, Mayer-Proschel M. Identifying a window of vulnerability during fetal development in a maternal iron restriction model. PLoS One. 2011;6:e17483.
34. World Health Organization. UNICEF: indicators for assessing, and strategies for preventing iron deficiency. Geneva, Switzerland: WHO; 1996.
35. Reeves TM, Phillips LL, Povlishock JT. Myelinated and unmyelinated axons of the corpus callosum differ in vulnerability and functional recovery following traumatic brain injury. Exp Neurol. 2005;196:126–37.
36. Zhou FM, Hablitz JJ. Morphological properties of intracellularly labeled layer I neurons in rat neocortex. J Comp Neurol. 1996;376:198–213.
37. Sholl DA. Dendritic organization in the neurons of the visual and motor cortices of the cat. J Anat. 1953;87:387–406.
38. Ennaceur A, Delacour J. A new one-trial test for neurobiological studies of memory in rats. 1: Behavioral data. Behav Brain Res. 1988;31:47–59.
39. Ennaceur A. One-trial object recognition in rats and mice: methodological and theoretical issues. Behav Brain Res. 2010;215:244–54.
40. Gaskin S, Tardif M, Cole E, Piterkin P, Kayello L, Mumby DG. Object familiarization and novel-object preference in rats. Behav Processes. 2010;83:61–71.
41. Preston RJ, Waxman SG, Kocsis JD. Effects of 4-aminopyridine on rapidly and slowly conducting axons of rat corpus callosum. Exp Neurol. 1983;79: 808–20.
42. Swanson J, Castellanos FX, Murias M, LaHoste G, Kennedy J. Cognitive neuroscience of attention deficit hyperactivity disorder and hyperkinetic disorder. Curr Opin Neurobiol. 1998;8:263–71.
43. Langhammer CG, Previtera ML, Sweet ES, Sran SS, Chen M, Firestein BL. Automated Sholl analysis of digitized neuronal morphology at multiple scales: whole cell Sholl analysis versus Sholl analysis of arbor subregions. Cytometry A. 2010;77:1160–8.
44. DeMaman AS, Homem JM, Lachat JJ. Early iron deficiency produces persistent damage to visual tracts in Wistar rats. Nutr Neurosci. 2008; 11:283–9.
45. DeMaman AS, Melo P, Homem JM, Tavares MA, Lachat JJ. Effectiveness of iron repletion in the diet for the optic nerve development of anaemic rats. Eye (Lond). 2010;24:901–8.
46. Koester SE, O'Leary DD. Axons of early generated neurons in cingulate cortex pioneer the corpus callosum. J Neurosci. 1994;14:6608–20.
47. Wu LL, Zhang L, Shao J, Qin YF, Yang RW, Zhao ZY. Effect of perinatal iron deficiency on myelination and associated behaviors in rat pups. Behav Brain Res. 2008;188:263–70.
48. Yu GS, Steinkirchner TM, Rao GA, Larkin EC. Effect of prenatal iron deficiency on myelination in rat pups. Am J Pathol. 1986;125:620–4.
49. Beard J, Tobin B, Green W. Evidence for thyroid hormone deficiency in iron-deficient anemic rats. J Nutr. 1989;119:772–8.
50. Waxman SG, Davis PK, Black JA, Ransom BR. Anoxic injury of mammalian central white matter: decreased susceptibility in myelin-deficient optic nerve. Ann Neurol. 1990;28:335–40.
51. Mayer-Pröschel M, Morath D, Noble M. Are hypothyroidism and iron deficiency precursor cell diseases? Dev Neurosci. 2001;23:277–86.
52. Beard JL, Wiesinger JA, Connor JR. Pre- and postweaning iron deficiency alters myelination in Sprague-Dawley rats. Dev Neurosci. 2003;25: 308–15.
53. Jorgenson LA, Wobken JD, Georgieff MK. Perinatal iron deficiency alters apical dendritic growth in hippocampal CA1 pyramidal neurons. Dev Neurosci. 2003;25:412–20.
54. Jorgenson LA, Sun M, O'Connor M, Georgieff MK. Fetal iron deficiency disrupts the maturation of synaptic function and efficacy in area CA1 of the developing rat hippocampus. Hippocampus. 2005;15:1094–102.
55. Klausberger T, Somogyi P. Neuronal diversity and temporal dynamics: the unity of hippocampal circuit operations. Science. 2008;321:53–7.
56. Wang GW, Cai JX. Disconnection of the hippocampal-prefrontal cortical circuits impairs spatial working memory performance in rats. Behav Brain Res. 2006;175:329–36.
57. Buckmaster CA, Eichenbaum H, Amaral DG, Suzuki WA, Rapp PR. Entorhinal cortex lesions disrupt the relational organization of memory in monkeys. J Neurosci. 2004;24:9811–25.